Elsevier Editorial System(tm) for Chemical Engineering Journal

Manuscript Draft

Manuscript Number:

Title: Simultaneous biological nitrous oxide abatement and wastewater treatment in a denitrifying off-gas bioscrubber

Article Type: Research Paper

Section/Category: Environmental Chemical Engineering

Keywords: N2O; wastewater treatment; EBRT; denitrification; biofiltration; greenhouse gas

Corresponding Author: Dr. Raul Munoz, PhD

Corresponding Author's Institution: Valladolid University

First Author: Osvaldo D Frutos, MSc

Order of Authors: Osvaldo D Frutos, MSc; Guillermo Quijano, PhD; Rebeca Pérez, PhD; Raul Munoz, PhD

Abstract: The simultaneous treatment of N2O-laden air emissions and domestic wastewater was assessed in a novel denitrifying bioscrubber composed of a packed bed absorption column interconnected to a fixed bed reactor (FBR). The influence of liquid recycling velocities and gas empty bed residence times (EBRT) in the absorption column on bioscrubber's performance was evaluated using synthetic wastewater (SW) and a 100 ± 8 ppmv N2O air emission. Steady state N2O removal efficiencies of 36 ± 3 % concomitant with SW total organic carbon removals of 91 ± 1 % were achieved at an EBRT of 3 min and at the highest UL tested (8 m h-1). The removal of dissolved N2O by heterotrophic denitrification in the FBR constituted the main N2O biodegradation mechanism and limited the abatement of N2O. While the supplementation of SW with Cu2+ (a cofactor of the N2O reductase) did not result in an enhancement in N2O reduction, the increase in FBR volume supported a higher N2O removal. The increase in EBRT up to 40 min supported an enhancement in the gas N2O removal of up to 92 %. The DGGE-sequencing analysis of FBR microbial population revealed a high microbial diversity and the abundance of denitrifying bacteria capable of reducing N2O to N2.

Suggested Reviewers: Eldon R. Rene
Lecturer in Resource Recovery Technology, UNESCO-IHE Institute for Water Education
e.raj@unesco-ihe.org
Specialist in biofiltration of VOCs and Wastewater treatment processes

Alberto Vergara Fernández
Facultad de Ingeniería y Ciencias Aplicadas, Universidad de los Andes
aovergara@miuandes.cl
Specialist in bioprocess, biofiltration and molecular biology

Jianjun Li

State Key Laboratory of Applied Microbiology, Guangdong Institute of Microbiology
lijianjun716@yahoo.com.cn
Specialist in biotrickling filtration

Opposed Reviewers:

Department of Chemical Engineering
and Environmental Technology
Valladolid University

Marc Deshusses
Chemical Engineering Journal
Editor

Dear Professor Deshusses,

Please find enclosed our unpublished original manuscript "**Simultaneous biological nitrous oxide abatement and wastewater treatment in a denitrifying off-gas bioscrubber**" co-authored by Osvaldo D. Frutos, Guillermo Quijano, Rebeca Pérez, and Raúl Muñoz. All authors are aware of the CEJ ethics policy, declare no conflict of interest and accept the responsibility for the present manuscript. This manuscript has been prepared according to the CEJ guide for authors.

The predicted environmental, social and economic consequences of global warming are causing an increasing concern about GHG emissions worldwide. Nitrous oxide ($N_2O$) constitutes one of the most powerful GHGs, which is typically emitted in wastewater treatment plants. Therefore, the minimization of $N_2O$ emissions has become one of the main challenges of WWTPs operators. In this context, the performance of an innovative anoxic bioscrubber for the simultaneous abatement of $N_2O$ emissions and wastewater treatment was evaluated. High removal efficiencies of $N_2O$ and organic carbon from wastewater were achieved following process optimization.

In order to avoid any potential conflict of interests based on the current good relationships between Spanish groups working in the field of biofiltration, the authors would highly appreciate the absence of Spanish researchers/academics in the peer-review of this work.

Based on the increasing relevance of anthropogenic GHG emissions and their implications on climate change, we strongly believe that this paper fits well in the scope of *Chemical Engineering Journal* and will certainly attract international attention.

We look forward to your evaluation.

Best regards,

**Raúl Muñoz** **Osvaldo D. Frutos**

*Postal address* 47005 Valladolid; *Visiting address* Paseo del Prado de la Magdalena s/n; *Telephone* +34983184934, *Fax* +34983423013; *E-mail* mutora@iq.uva.es; *Internet* http://www.iq.uva.es

**Recommended reviewers:**

**Eldon R. Rene**
UNESCO-IHE Institute for Water Education. Lecturer in Resource Recovery Technology.
Tel.: +31152151840
Email: e.raj@unesco-ihe.org

**Alberto Vergara Fernández**
Facultad de Ingeniería y Ciencias Aplicadas, Universidad de los Andes, Chile
Email: aovergara@miuandes.cl

**Jianjun Li**
Guangdong Institute of Microbiology, Guangzhou 510070, China
Email: lijianjun716@yahoo.com.cn

Graphical Abstract (for review)

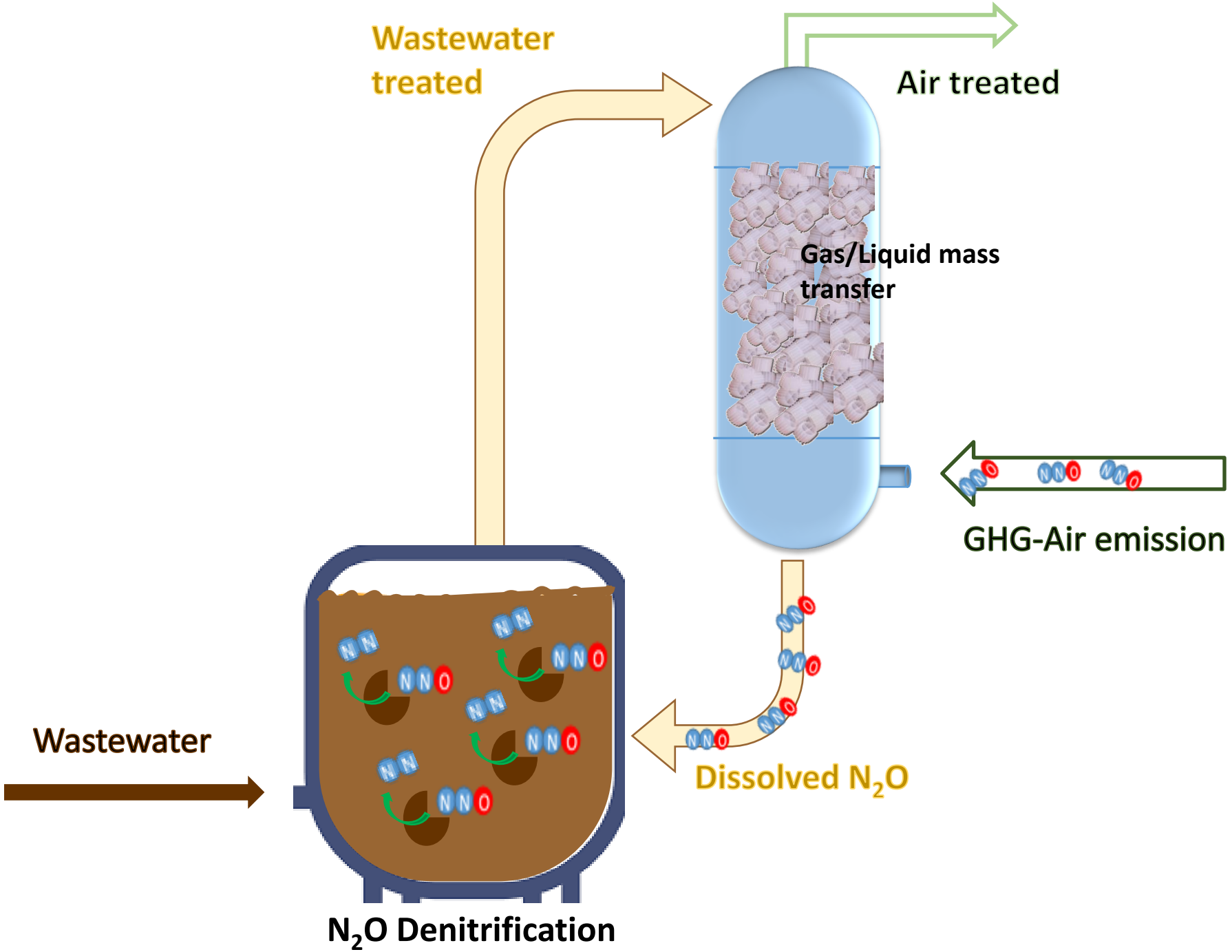

## Highlights

- The potential of an innovative anoxic bioscrubber for $N_2O$ abatement was evaluated.
- The simultaneous $N_2O$ abatement and wastewater treatment was feasible.
- Higher $N_2O$ removals supported by increasing liquid recycling velocities and EBRTs.
- $N_2O$ removal efficiencies of 92 % were achieved at an EBRT of 40 min.
- Efficient organic carbon removals (85-95%) from wastewater were recorded.

# Simultaneous biological nitrous oxide abatement and wastewater treatment in a denitrifying off-gas bioscrubber

*Osvaldo D. Frutos*[†, ‡], *Guillermo Quijano*[†], *Rebeca Pérez*[†], *Raúl Muñoz*[*†]

† Department of Chemical Engineering and Environmental Technology, University of Valladolid, Dr. Mergelina, s/n, 47011, Valladolid, Spain. Tel. +34 983186424, Fax: 983423013.

‡ Facultad de Ciencias Agrarias, Universidad Nacional de Asunción, Campus San Lorenzo, Paraguay

*-Author for correspondence: mutora@iq.uva.es

## Abstract

The simultaneous treatment of $N_2O$-laden air emissions and domestic wastewater was assessed in a novel denitrifying bioscrubber composed of a packed bed absorption column interconnected to a fixed bed reactor (FBR). The influence of liquid recycling velocities and gas empty bed residence times (EBRT) in the absorption column on bioscrubber's performance was evaluated using synthetic wastewater (SW) and a 100 ±

8 $ppm_v$ $N_2O$ air emission. Steady state $N_2O$ removal efficiencies of 36 ± 3 % concomitant with SW total organic carbon removals of 91 ± 1 % were achieved at an EBRT of 3 min and at the highest $U_L$ tested (8 m $h^{-1}$). The removal of dissolved $N_2O$ by heterotrophic denitrification in the FBR constituted the main $N_2O$ biodegradation mechanism and limited the abatement of $N_2O$. While the supplementation of SW with $Cu^{2+}$ (a cofactor of the $N_2O$ reductase) did not result in an enhancement in $N_2O$ reduction, the increase in FBR volume supported a higher $N_2O$ removal. The increase in EBRT up to 40 min supported an enhancement in the gas $N_2O$ removal of up to 92 %. The DGGE-sequencing analysis of FBR microbial population revealed a high microbial diversity and the abundance of denitrifying bacteria capable of reducing $N_2O$ to $N_2$.

**Keywords**

$N_2O$, wastewater treatment, EBRT, denitrification, biofiltration, greenhouse gas

# 1 Introduction

Nitrous oxide ($N_2O$) is one of the major greenhouse gases (GHG) emitted nowadays, which contributes to climate change with a 6.2 % of the total GHG emissions due to its high global warming potential (≈300 times higher than that of $CO_2$) [1]. $N_2O$ is also considered the most important $O_3$-depleting substance emitted in this XXI century [2]. In Europe, $N_2O$ is mainly emitted from agriculture (268300 Gg of $CO_2$ eq), wastewater treatment processes (12299 Gg of $CO_2$ eq) and adipic and nitric acid production (9682 Gg of $CO_2$ eq) [3]. In wastewater treatment plants (WWTPs), $N_2O$ is mainly produced during biological nitrogen removal, with nitrifier denitrification, heterotrophic denitrification and hydroxylamine oxidation as the main routes of $N_2O$ production in activated sludge processes [4]. Some authors have also reported $N_2O$ emissions during wastewater biofiltration [5, 6], where $N_2O$ production was mainly associated to nitrification and denitrification processes. Even new microbial nitrogen removal processes such as nitritation/anammox or SHARON emit significant amounts of $N_2O$ [7, 8].

Based on the renovated and more ambitious EU objective for the reduction of the European GHG emissions by 40 % in 2030 (compared to 1990 levels) [9], the minimization of $N_2O$ emissions from wastewater treatment has become one of the main challenges of WWTP operators in this XXI century. In this regard, physical/chemical technologies such as thermal decomposition, selective catalytic reduction and selective non-catalytic reduction, typically used for industrial NOx emission abatement, could be applied as end-of-the-pipe technologies in WWTPs. However, these technologies entail the consumption of costly and/or hazardous chemicals, process operation at high temperatures and the generation of secondary pollution, which results in high operating costs and environmental impacts [10]. On the other hand, biotechnologies have been

consistently shown as an environmentally friendly and low cost alternative for off-gas treatment, which exhibit a robustness and efficiency comparable to that of their physical/chemical counterparts [11]. Unfortunately, despite some works on $NO/NO_2$ nitrification and denitrification have been carried out [12, 13], the number of studies assessing the potential of biotechnologies for $N_2O$ abatement is scarce. This GHG is an obligate intermediate during the anoxic nitrogen reduction ($NO_3^- \rightarrow NO_2^- \rightarrow NO \rightarrow N_2O \rightarrow N_2$), which up to date has been reported as the only biological $N_2O$ removal mechanism. Therefore, the removal of $N_2O$ from air emissions entails the need for bioreactor configurations involving a $N_2O$ absorption step in water followed by a $N_2O$ reduction step under anaerobic conditions. The maintenance of anaerobic conditions in the denitrification tank requires the external supply of a carbon source (e.g. methanol) to biologically deplete all $O_2$ present in the $N_2O$-laden aqueous stream, with the subsequent increase in process operating costs [14]. Therefore, innovative operational strategies based on the use of free carbon sources such as wastewater in WWTPs must be developed in order to achieve cost-effective $N_2O$ removal processes.

The aim of this work was to evaluate the feasibility of the simultaneous $N_2O$ abatement and wastewater treatment in a lab-scale bioscrubber consisting of a packed bed absorption column coupled to a denitrifying fixed bed bioreactor. The influence of liquid recycling velocities and gas empty bed residence times on the removal of $N_2O$ and wastewater treatment performance was also investigated.

# 2 Materials and methods

## 2.1 Chemicals and Synthetic Wastewater

A 40 L calibration gas mixture of 10000 $ppm_v$ of $N_2O$ in $N_2$ was purchased from Abelló Linde S.A. (Barcelona, Spain). The synthetic wastewater (SW) used in the

experimentation was composed of (in g $L^{-1}$ of tap water): peptone 0.16, meat extract 0.11, urea 0.03, NaCl 0.007, $CaCl_2 \cdot 2H_2O$ 0.004, $MgSO_4 \cdot 7H_2O$ 0.002, $K_2HPO_4$ 0.028, $CuCl_2 \cdot 2H_2O$ $50 \times 10^{-6}$ and glucose 0.25. The final concentrations of total organic carbon (TOC), total nitrogen (TN) and $PO_4^{3-}$ of the SW were 256.1 ± 22.7, 54.4 ± 2.9 and 11.7 ± 3.3 mg $L^{-1}$, respectively. All reagents were purchased from PANREAC with a purity of +99 % (Barcelona, Spain). The biodegradability of the SW was experimentally determined in independent batch assays by monitoring the TOC and TN concentrations for 14 days in three 500 mL Erlenmeyer initially filled with 99 mL of sterilized SW and 1 mL of activated sludge from Valladolid WWTP (Spain). Two non-inoculated sterilized Erlenmeyer with 100 mL of SW were used as controls to elucidate any potential carbon or nitrogen abiotic removal.

### 2.2 Experimental set up

A lab-scale bioscrubber was set up for the continuous abatement of a diluted air emission of $N_2O$ and the simultaneous treatment of SW for 140 days. The experimental system was composed of a $N_2O$ absorption column made of PVC and packed with 2 L of Kaldnes rings interconnected with a 3 L fixed bed bioreactor (FBR) (Afora S.A., Spain). The FBR was filled with 1 L of methylotrophs-containing polyurethane foam (PUF) cubes (1 $cm^3$) used in a previous experiment as the packed bed of an absorption column [14]. The FBR was constructed with a 0.55 L liquid distribution chamber located at the bottom of the tank and operated with magnetic stirring at 300 rpm (Fig. 1). The experimental set-up was located in an air-conditioned room at 25 ºC. Prior to inoculation, an abiotic test was performed with tap water for 4 days in order to assess any potential removal of $N_2O$ by adsorption or photodegradation in the experimental set-up.

<Fig. 1.>

## 2.3 Bioscrubber operation

The SW was introduced at the bottom of the FBR, where it mixed with the $N_2O$-laden recycling liquid from the absorption column, and was further recirculated from the top of the FBR to the top of the packed bed absorption column using a peristaltic pump (Watson Marlow, UK). The $N_2O$-laden air emission was introduced at the bottom of the absorption column flowing upwards counter currently with the recycling liquid. The synthetic $N_2O$-laden air inflow was obtained by mixing 660 mL $min^{-1}$ of air and 6.7 mL $min^{-1}$ of the 10000 $ppm_v$ $N_2O$ calibration gas mixture using a mass flow controller (Aalborg, Denmark), resulting in a gas empty bed residence time (EBRT) in the absorption column of 3 min and a $N_2O$ concentration of 100 ± 8 $ppm_v$, which correspond to typical off-gas emissions from WWTPs. The SW was supplied to the FBR at flow rates determined by the maintenance of anoxic conditions (targeting a dissolved oxygen concentration = 0 mg $L^{-1}$) in the FBR. No $N_2O$ was supplied to the inlet air for the first 18 days of operation (stage I) in order to assess any potential $N_2O$ generation in the system as a result of wastewater treatment. During stage I, the bioscrubber was operated with a SW flow rate of 3 ± 0.1 L $d^{-1}$ and a liquid recycling velocity ($U_L$) of 1 m $h^{-1}$. Stage II (days 19-51) was characterized by process operation at a $N_2O$ of 100 ± 8 $ppm_v$, $U_L$ of 1 m $h^{-1}$ and a SW flow rate of 4 ± 1 L $d^{-1}$. $U_L$ was increased up to 4 m $h^{-1}$ during stage III (days 52-83) concomitantly with an increase in SW flow rate to 19 ± 1 L $d^{-1}$. The bioscrubber was operated from day 84 to 104 (stage IV) with a $U_L$ of 8 m $h^{-1}$ and a SW flow rate of 36 ± 4 L $d^{-1}$. Similar SW flow rates and $U_L$ were maintained during stage V (days 105-118), which was characterized by the supplementation to the SW of $CuCl_2 \cdot 2H_2O$ at 50 μg $Cu^{2+}$ $L^{-1}$ in order to assess the influence of copper (a cofactor of the nitrous oxide reductase) on $N_2O$ degradation.

Finally, the 3L-FBR volume was substituted by a new 7.5L-FBR in stage VI (days 119-135) in order to enhance $N_2O$ reduction under process operation at a $U_L$ of 8 m $h^{-1}$ and a SW flow rate of 38 ± 1 L $d^{-1}$. The packed bed of the initial FBR, plus 4 L of new PUF cubes, constituted the packing medium of the 7.5 L FBR. From day 136 to 140, the EBRT was stepwisely increased to 6, 12, 18, 40 and 80 min under the operational conditions set in stage VI.

Liquid samples from the SW at FBR inlet, and inlet and outlet of the absorption column were periodically drawn to determine the concentration of $NO_2^-$ and $NO_3^-$. TOC, inorganic carbon (IC) and TN concentrations were also measured in the SW inlet and effluent of FBR. The $N_2O$ and $CO_2$ gas concentrations at the inlet and outlet of the absorption column were determined by GC-ECD and GC-TCD, respectively. In addition, the aqueous $N_2O$ concentration of the recycling liquid was measured by headspace GC-ECD at the inlet and outlet of the FBR to assess the denitrification capacity of the system. All measurements were carried out three times a week. The biomass concentration as total suspended solids (TSS) and the dissolved reactive orthophosphate ($PO_4^{-3}$) concentration were also measured in the SW and bioscrubber effluent under steady state conditions.

### 2.4 Analytical procedures

The $N_2O$ and $CO_2$ gas concentration were measured by GC-ECD and GC-TCD according to Frutos et al. [14] and López et al. [15], respectively. The aqueous $N_2O$, TOC, IC, TN and $O_2$ concentrations were determined following the methodology described in Frutos et al. [14]. $NO_2^-$, $NO_3^-$ and $PO_4^{3-}$ were measured colorimetrically in a UV-2550 spectrophotometer (Shimadzu, Tokyo, Japan) according the Standard Methods 4500-$NO_2^-$ B, 4500-$NO_3^-$ E and 4500-P C, respectively [16].

## 2.5 Molecular biology analysis

Samples of biomass from the methylotrophs-containing PUF used as inoculum and from the biomass entrapped in the PUF of the 7.5 L FBR at the end of the experimentation (day 140) were stored immediately at -20 ºC to assess the diversity and composition of the microbial community. The genomic DNA was extracted according Lebrero et al. [17]. The PCR mixture was composed of 25 µL of BIOMIX ready-to-use 2× reaction mix (Bioline, Ecogen), 2 µL of the extracted DNA, 2 µL of the PCR primers 968-F-GC and 1401-R (10 µM) (Sigma-Aldrich, St. Louis, MO, USA) for bacterial 16S rRNA gene amplification, and Milli-Q water up to a final volume of 50 µL. The PCR thermo-cycling program used and the DGGE analysis was previously described in Lebrero et al. [17]. The gels were stained with GelRed Nucleic Acid Gel Stain (biotium) for 1 h 30 min and the obtained DGGE patterns processed using the GelCompar IITM software (Applied Maths BVBA, Sint-Martens- Latem, Belgium). Similarity indices of the compared profiles were calculated from the densitometric curves of the scanned DGGE profiles by using the Pearson product–moment correlation coefficient [18]. The peak heights in the densitometric curves were also used to determine the Shannon–Wiener diversity index (H).

The most relevant bands were excised from the DGGE gel and the procedure was previously described in Lebrero et al. [17]. The taxonomic position of the sequenced DGGE bands was obtained using the RDP classifier tool (50 % confidence level) [19]. The closest matches to each band were obtained using the BLAST search tool at the NCBI (National Centre for Biotechnology Information) [20]. Sequences were deposited in GenBank Data Library under accession numbers KT200317-KT200331.

### 2.6 Statistical analysis

Results from the bioscrubber performance were evaluated using a parametric Student's t-test and Kruskal Wallis ANOVA non-parametric tests, both at 95 % confidence level to assess any significant influence of the operational conditions tested on process parameters.

## 3 Results

No significant $N_2O$ removal (<2 %) by adsorption or photolysis was observed during the 4-days abiotic test. The average error in $N_2O$ measurements by GC-ECD was 2.1 % and therefore any potential $N_2O$ degradation was attributed to microbial activity. The pH of the bioscrubber during the 140 days of biotic operation remained roughly constant at 7.3 ± 0.2. $N_2O$ gas concentrations of 1 ± 1 $ppm_v$ were recorded at the outlet of the absorption column during the first 18 days of operation in the absence of $N_2O$ supply at a $U_L$ of 1 m $h^{-1}$ (Fig. 2a). The determination of the aqueous $N_2O$ during this stage I showed higher concentrations at the inlet (46 ± 16 µg $N_2O$ $L^{-1}$) than at the outlet of the FBR (15 ± 4 µg $N_2O$ $L^{-1}$) (Fig. 2b). Steady state TOC and TN removal efficiencies of 90 ± 5 % and 75 ± 15 % were recorded, respectively (Fig. 3a and 3c). This TOC removal resulted in elimination capacities (ECs) of 184 ± 24 g C $m^{-3}$ $d^{-1}$ and $CO_2$ gas production rates of 138 ± 8 g C $m^{-3}$ $d^{-1}$ (Fig. 3b). Steady state $NO_3^-$ concentrations in the inlet SW, effluent of the FBR and outlet of the absorption column accounted for 0.93 ± 0.17, 0.13 ± 0.05 and 0.55 ± 0.31 mg N $L^{-1}$, respectively (Fig. S1). Likewise, $NO_2^-$ concentrations of 0.07 ± 0.06, 0.39 ± 0.20 and 1.27 ± 0.51 mg N $L^{-1}$ were recorded in the SW, effluent of the FBR and outlet of the absorption column (Fig. S1).

<Fig. 2.>

Process operation at an inlet $N_2O$ gas concentration of 100 ± 8 $ppm_v$ and a $U_L$ of 1 m $h^{-1}$ during stage II was characterized by a steady gas $N_2O$ removal efficiency (RE) of 8 ± 3 % (Fig. 2a). Under these particular conditions, an efficient dissolved $N_2O$ removal by anoxic denitrification in the FBR was observed (65 ± 16 %) (Fig. 2b). An increase in the TOC-RE up to 95 ± 3 % was recorded, which corresponded to an EC of 327 ± 35 g C $m^{-3}$ $d^{-1}$ and a $CO_2$ production rate of 277 ± 43 g C $m^{-3}$ $d^{-1}$. Likewise, TN-RE during stage II reached 90 ± 2 % (Fig. 3c). $NO_3^-$ concentrations in the SW, effluent of the FBR and outlet of the absorption column remained constant during stage II at 0.92 ± 0.18, 0.46 ± 0.26 and 0.76 ± 0.35 mg N $L^{-1}$, respectively (Fig. S1). Likewise, $NO_2^-$ concentrations of 0.04 ± 0.02, 0.37 ± 0.47 and 0.30 ± 0.40 mg N $L^{-1}$ were recorded at the above referred sampling points (Fig. S1). Finally, $PO_4^{3-}$ removal efficiency under steady state accounted only for 21 %, which resulted in effluent concentrations of 7.3 mg P $L^{-1}$ (Table S1). Negligible TSS concentrations were observed in the FBR effluent at the end of stage II (e.g. less than 0.1 mg $L^{-1}$).

<Fig. 3.>

The increase in $U_L$ to 4 m $h^{-1}$ during stage III entailed an enhancement in the gas $N_2O$ degradation up to steady state REs of 17 ± 2 % (Fig. 2a). The reduction to $N_2$ of the aqueous $N_2O$ in the FBR remained significantly similar at 60 ± 10 % despite the increase in $U_L$ (Fig. 2b). However, a slight but significant decrease in the TOC removal efficiency was recorded (89 ± 4 %) along with the increase in the SW flow rate to 19 ± 1 L $d^{-1}$ (Fig. 3a). This increase in the SW loading rate resulted in an increase of TOC-EC up to 1503 ± 131 g C $m^{-3}$ $d^{-1}$ and in a $CO_2$ production rate of 667 ± 66 g C $m^{-3}$ $d^{-1}$ (Fig. 3b). A severe decrease in the steady state TN removal efficiency to 40 ± 9 % was

observed (Fig. 3c). Under these particular conditions, the concentrations of $NO_3^-$ in the SW, effluent of the FBR and outlet of the absorption column at steady state were 0.77 ± 0.27, 0.04 ± 0.08 and 0.04 ± 0.08 mg N $L^{-1}$, respectively, while $NO_2^-$ concentrations were negligible (Fig. S1). Finally, despite the removal efficiency of $PO_4^{3-}$ increased up to 49 ± 1 %, the effluent concentration remained at 8.5 ± 1 mg P $L^{-1}$ as a result of the increase in SW phosphorus concentration to 16.6 ± 0.1 mg P $L^{-1}$. The concentrations of TSS in the effluent during stage III were 0.08 ± 0.01 g $L^{-1}$ (Table S1).

An increase in the steady state gas $N_2O$ RE up to 26 ± 5 % (Fig. 2a), concomitant with a deterioration in the $N_2O$ denitrification efficiency in the FBR to 38 ± 12 %, was recorded along with the increase in $U_L$ to 8 m $h^{-1}$ (Fig. 2b) in stage IV. The increase in the SW flow rate up to 36 ± 4 L $d^{-1}$ in order to maintain anoxic conditions in the FBR mediated a decrease in the TOC-RE (Fig. 3a) to 85 ± 4 %, which corresponded to an EC and a $CO_2$ production rate of 2599 ± 95 and 992 ± 103 g C $m^{-3}$ $d^{-1}$, respectively (Fig. 3b). Nevertheless, TN removal showed no significant variation under steady state conditions during stage IV (43 ± 4 %) (Fig. 3c). $NO_3^-$ and $NO_2^-$ were only detected in the SW at 0.46 ± 0.33 mg N $L^{-1}$ and 0.07 ± 0.06 mg N $L^{-1}$, respectively (Fig. S1). The increase in SW flow rate resulted in $PO_4^{3-}$ removal efficiencies of 52 ± 6 % and in an increase in TSS effluent concentration up to 0.14 ± 0.04 g $L^{-1}$ (Table S1).

The addition of $CuCl_2 \cdot 2H_2O$ to the SW by day 105 supported steady state gas $N_2O$ REs of 29 ± 2 % and $N_2O$ denitrification efficiencies of 38 ± 9 % in the FBR. The removal efficiencies of TOC and TN during stage V remained constant at 87 ± 2 and 40 ± 3 %, respectively (Fig. 3a and 3c) in spite of the increase in SW flow rate to 37 ± 1 L $d^{-1}$. The $CO_2$ production rate and TOC-EC under steady state conditions were 1112 ± 82 g C $m^{-3}$ $d^{-1}$ and 2732 ± 179 g C $m^{-3}$ $d^{-1}$, respectively (Fig. 3b). $NO_3^-$ and $NO_2^-$ were only detected in the SW at 0.20 ± 0.05 and 0.28 ± 0.12 mg N $L^{-1}$ (Fig. S1), respectively. The $PO_4^{3-}$

removal efficiency of the FBR during stage V reached 58 ± 13 % and resulted in effluent concentrations of 3.7 ± 1 mg P $L^{-1}$. On the other hand, TSS concentrations in the SW and effluent were 0.04 ± 0.02 and 0.12 ± 0.04 g $L^{-1}$, respectively (Table S1).

Finally, the increase in the volume of FBR from 3 L to 7.5 L during stage VI brought about a gas $N_2O$ RE of 36 ± 3 % and an increase in the removal of the aqueous $N_2O$ up to 63 ± 4 % in the FBR. A TOC removal efficiency of 91 ± 1 % was recorded under steady state operation (Fig. 3a) along with an EC of 1133 ± 51 g C $m^{-3}$ $d^{-1}$. Likewise, a decrease of $CO_2$ production rate up to 482 ± 12 g C $m^{-3}$ $d^{-1}$ was observed (Fig. 3b). The recorded TN-RE remained at 42 ± 5 % (Fig. 3c). Negligible concentrations of $NO_3^-$ and $NO_2^-$ were recorded at the FBR effluent and in the outlet of the absorption column (Fig. S1) whereas the $NO_3^-$ and $NO_2^-$ concentrations in the SW were 0.32 ± 0.18 and 0.27 ± 0.20 mg N $L^{-1}$, respectively. $PO_4^{3-}$-REs remained at 57 ± 7 % with effluent concentrations of 4.3 ± 0.2 mg P $L^{-1}$. The TSS effluent concentration decreased to 0.06 ± 0.01 g $L^{-1}$ in this last stage.

<Fig. 4.>

Process operation at an EBRT of 3 min supported a gas $N_2O$-RE of 36 ± 0.2 % along with dissolved $N_2O$ and TOC removals of 69 ± 1 and 92 %, respectively. The stepwise increase in gas EBRT in the absorption column resulted in a sequential enhancement in the gas $N_2O$-REs but in a deterioration of the removal efficiencies of aqueous $N_2O$ and TOC (Fig. 4). Hence, the highest gas $N_2O$-RE (94 ± 0.2 %) was achieved at an EBRT of 80 min along with TOC and dissolved $N_2O$ removal efficiencies of 74 % and 17 ± 2 %, respectively (Fig. 4).

<Fig. 5.>

The Shannon-Wiener diversity indices of the microbial communities present in the inoculum and at the end of the experimental period were 3.48 and 3.47, respectively (Fig. 5). The initial and final bacterial populations were analyzed using the Pearson similarity correlation coefficient in order to elucidate the structure of the bacterial communities in the FBR. A similarity value of 11.7 % was obtained between the communities present at day 0 and day 140. From the DGGE gel, 15 bands were sequenced (Fig. 5) and 4 different phyla were identified from the RDP database: *Proteobacteria* (11 bands), *Firmicutes* (2 bands), *Lentisphaerae* (1 band) and *Cloacimonetes* (1 band). The closest matches for every band (BLASTN) according to the NCBI database, together with its similarity percentages and sources of origin, are provided as supplementary material (Table S2).

## 4 Discussion

This work demonstrated the feasibility of a simultaneous removal of $N_2O$ from WWTP air emissions coupled to wastewater treatment using an innovative absorption unit-anoxic tank bioscrubber configuration. $N_2O$ removal was based on the sequential $N_2O$ mass transfer from the gas to the recycling liquid in the packed bed column followed by $N_2O$ reduction under anoxic conditions in the FBR using the organic matter present in the SW as electron donor. The sole degradation mechanism of $N_2O$ was heterotrophic denitrification in the FBR, while no significant $N_2O$ biodegradation was observed in the absorption column likely due the high $O_2$ levels in the air emission.

$N_2O$ production was observed in the first operational stage (Fig. 2), which could be attributed to the oxidation of the hydroxylamine produced by the action of ammonium oxidizing bacteria in the absorption column [4]. The sequential increase of $U_L$ mediated the enhancement in the gas $N_2O$ RE as a result of the higher turbulence in the gas/liquid

interface (which likely increased the $N_2O$ mass transfer coefficients [21]) and the higher $N_2O$ carry over capacity of the recycling liquid. Hence, the increase in $U_L$ entailed a higher aqueous $N_2O$ loading rate to the FBR since the dissolved $N_2O$ concentration at the outlet of the absorption column was close to saturation regardless of the operational conditions. However, it is worth noting that this stepwise increase in $U_L$ deteriorated the dissolved $N_2O$ removal in the 3 L FBR likely due to its associated decrease in the recycling liquid residence times from 32 min at a $U_L$ of 1 m $h^{-1}$ to 4 min at a $U_L$ of 8 m $h^{-1}$. Thus, the dissolved $N_2O$ removal efficiency dropped from 65 ± 16 % in stage II to 38 ± 9 % in stage V (Fig. 2b), corresponding to the lowest and highest $U_L$ evaluated in the bioscrubber, respectively. This deterioration in the dissolved $N_2O$ removal likely caused the low gas $N_2O$ RE of 29 ± 2 % recorded in stage V as a result of the low gas-liquid $N_2O$ concentration gradient (Fig. 2a). In this context, the 3 L FBR was replaced by a 7.5 L FBR in stage VI in order to deplete all dissolved $N_2O$ in the anoxic tank, which would allow operating the absorption column at a maximum concentration gradient. The higher recycling liquid residence time in the 7.5 L FBR (≈10 min) promoted an increase in the dissolved $N_2O$ REs up to 63 ± 4 % (Fig. 2b), which consequently resulted in the enhancement of the gas $N_2O$ REs up to 36 ± 3 % (Fig. 2a). Copper is a structural component of the nitrous oxide reductase, the enzyme supporting the final reduction step of $N_2O$ to dinitrogen in the bacterial denitrification pathway [22]. In our particular study, $Cu^{2+}$ supplementation to the SW from stage V onward did not induce any significant improvement in $N_2O$ reduction in the anoxic tank. Conversely, Zhu et al. [23] did observe a decrease in $N_2O$ production by 55-73 % following the addition of 50-100 µg $Cu^{2+}$ $L^{-1}$ in a 4 L anaerobic–aerobic–anoxic sequencing batch reactor treating municipal wastewater. Overall, the $N_2O$ removal performance of this innovative bioscrubber configuration was likely limited by the poor

mass transfer of the pollutant from the air emission to the liquid phase in the absorption column due the low aqueous solubility of $N_2O$ ($H$ = 1.6 at 25 ºC [24]) and also to the low biological denitrification efficiency of the dissolved $N_2O$ mediated by the low residence time of the recycling liquid in the anoxic tank.

The wastewater treatment performance of the bioscrubber was characterized by high TOC removals, similar to the maximum biodegradability (96 %) of the SW used as a model wastewater (determined in an independent set of experiments). $O_2$, $N_2O$, $NO_2^-$ and $NO_3^-$ were simultaneously used as electron acceptors to support TOC oxidation in the FBR. A slight deterioration in TOC-RE was observed in spite of the sequential increase in SW flow rate to maintain the anoxic conditions needed for $N_2O$ reduction in the FBR, which resulted in a decrease in the hydraulic retention time (HRT) of the wastewater in bioscrubber (29, 19, 4, 2, 2 and 5 h for stages I, II, III, IV, V and VI, respectively). For instance, TOC effluent concentrations increased from 19 ± 11 mg C $L^{-1}$ in stage II to 29 ±11 and 31 ± 11 mg C $L^{-1}$ in stages III and IV, respectively (Fig. 3a). These effluent TOC concentrations remained below the maximum discharge limits required by European legislation [EU, 25], which demands a BOD effluent concentration of 25 mg $L^{-1}$ (≈70 mg C $L^{-1}$ based on a typical BOD/TOC ratio of 0.35 for treated wastewater [26]). On the other hand, while $Cu^{2+}$ supplementation did not influence the TOC-REs, the increase in the FBR volume in stage VI supported superior TOC-REs due to the HRT increase from 2 to 5 h. At this point it is important to highlight that a high TOC removal efficiency in the FBR is desirable to avoid biomass overgrowth in the absorption column, which punctually resulted in a reduction of the effective gas/liquid interfacial area and thus in a progressive deterioration of the $N_2O$ mass transfer capacity of the packed bed. Despite TOC-REs slightly decreased with increasing SW flow rates, the EC of the bioscrubber increased from 327 ± 35 g C $m^{-3}$ $d^{-1}$

in stage I to 2732 ± 179 g C $m^{-3}$ $d^{-1}$ in stage V, which confirmed the potential for organic matter treatment of the technology here evaluated. Similarly, $CO_2$ production rates increased concomitantly with the increase in EC (Fig. 3b). Carbon mineralization ratios of ≈82 % were recorded in the two first operational stages, while the sequential decrease in the HRT of the FBR resulted in a ≈53 % of the carbon mineralization ratio.

Nitrogen assimilation into microbial biomass and, in a much lesser extent, ammonium nitrification in the absorption column coupled with denitrification of the produced $NO_3^-$ and $NO_2^-$ in the anoxic tank were the main processes governing TN removal in the bioscrubber. These mechanisms occurred simultaneously in the two first operational stages, where nitrification in the absorption column supported the high TN removals observed (Fig. 3c, Fig. S1). Furthermore, ammonia stripping in the absorption column cannot be ruled out since the wastewater fed into the FBR was recycled at least 45 times/day through the absorption column during process operation at a HRT of ≈1 day and at a $U_L$ of 1 m $h^{-1}$. The increase in $U_L$ to 4 m $h^{-1}$ lowered the TN-RE of the system, which remained at ≈40 % from stage III onward (regardless of $Cu^{2+}$ supplementation and FBR volume increase), matching the N requirement for cell growth. Effluent TN concentrations of 14 ± 8 mg N $L^{-1}$ and 6 ± 1 mg N $L^{-1}$, which complied with the EU regulatory effluent values of 15 mg N $L^{-1}$ [EU, 25], were recorded in stages I and II, but remained above 30 mg N $L^{-1}$ from stage III onward (Fig. 3c). The good denitrification performance of the FBR supported low effluent $NO_2^-$ and $NO_3^-$ concentrations throughout the entire experimentation (Fig. S1). Finally, phosphorus removal efficiencies remained at ≈50 % over the entire experimental period (except during stage II), with effluent concentrations higher than the maximum permissible concentrations established by EU regulations (2 mg P $L^{-1}$) (Table S1). The concentrations of TSS in the effluent increased over the time course of the experimentation (Table S1) likely due to

the accumulation of biomass in the PUF of the FBR and the higher shear stress mediated by the sequential increase in liquid recycling. A reduction in the effluent TSS concentration was observed as a result of the FBR volume increase to 7.5 L (Table S1). Overall, despite the effluent concentrations of TN, phosphorus and TSS were often higher than those recommended by EU regulations for direct wastewater discharge, the technology here evaluated represents a cost effective pre-treatment unit, whose effluent can be returned back to the WWTP headworks or conducted to maturation ponds for tertiary treatment.

The stepwise increase in the EBRT of the air emission confirmed the potential of this innovative anoxic bioscrubber to simultaneously achieve high $N_2O$, organic matter and nutrient removal efficiencies (Fig. 4). A gradual increase in the gas $N_2O$ RE at increasing EBRTs was observed, with process operation at 80 min of EBRT supporting the highest $N_2O$ removals. On the contrary, this increase in the EBRT induced a deterioration in the removal of both TOC and aqueous $N_2O$ (Fig. 4), probably due to the decrease in the loading rate of electron acceptors ($O_2$ and $N_2O$) in the FBR, as confirmed by the lower aqueous $N_2O$ concentrations at the FBR inlet at increasing EBRTs (from 105 μg $N_2O$ $L^{-1}$ at an EBRT of 3 min to 26 μg $N_2O$ $L^{-1}$ at an EBRT 80 min). The in-situ generation of $N_2O$ in the system prevented the complete abatement of $N_2O$. Thus, process operation at an EBRT of 40 min and a $U_L$ of 8 m $h^{-1}$ was here identified as the optimal operating conditions, supporting $N_2O$ and TOC removals of 92 % and 81 %, respectively (Fig. 4). To the best of our knowledge, the REs here obtained under continuous operation were the highest so far reported in literature. In this context, Akdeniz et al. [27] reported a 0.7 % $N_2O$ removal efficiency in a lava rock media biofilter inoculated with swine manure and compost, and operated at an EBRT of 5 s. Likewise, Hood et al. [28] operated a biofilter composed of 70 % compost and 30 %

wood chips to treat the exhaust air from a swine barn pit ventilation fan at an EBRT of 7.6 s, with $N_2O$ removal efficiencies of 14-17 % at an inlet concentration of ≈170 $ppm_v$. In our particular study, the high EBRTs required to achieve high $N_2O$ REs would result in large bioscrubber volumes (with the subsequent increase in capital costs), which highlights the need for research on innovative cost-effective $N_2O$ mass transfer enhancement strategies.

The Shannon-Wiener diversity index takes into account both the number (richness) and the evenness of the species (by evaluating and comparing the intensity of the bands), allowing to obtain semi-quantitative results from the DGGE analysis (Table S2). Typical values ranging from 1.5 to 3.5 correspond to low and high species evenness and richness, respectively [29]. Thus, the diversity indices of the inoculum and the community present in the FBR at the end of the experimental period showed a high species evenness and diversity (Fig. 5). However, a low similarity between both microbial communities was observed likely due to the different electron donor used in this study (synthetic wastewater) compared with that used in the bioscrubber previously hosting the inoculum (methanol). Three families were the most abundant microbial communities (Table S2) in the inoculum sample: i) the *Xanthomonadaceae* family (DGGE band 3), with the capacity to carry out the full heterotrophic denitrification pathway [30], ii) the *Xanthobacteraceae* family (DGGE band 8), with the genus *Xanthobacter* which is strictly aerobic and can grow chemoorganoheterotrophically in methanol [31], and iii) the stricter anaerobic *Victivallaceae* family (DGGE band 14), with three uncultured species of the genus *Victivallis* [32]. Many species of the *Aeromonas* genus (DGGE bands 1-2 and 4-6), which possess the enzymatic machinery to denitrify $N_2O$ under aerobic conditions, were observed in the final community present in the FBR (Table S2) at the end of the experimentation [33]. Furthermore, the

abundance of denitrifiers *Aquaspirillum* related species (DGGE band 10) in the FBR agreed with previous studies where these denitrifying *Betaproteobacteria* were found in municipal activated sludge [34]. Finally, the presence of *Clostridium sensu stricto* and *Candidatus cloacamonas* related bacteria (DGGE bands 12 and 14, respectively) and anaerobic species from the order *Selenomonadales* (DGGE band 13) suggested the occurrence of anaerobic niches in the FBR.

## 5 Conclusions

In brief, the simultaneous treatment of both $N_2O$-laden air emissions and wastewater was achieved in this innovative absorption unit-anoxic tank bioscrubber configuration. Higher gas $N_2O$ REs were recorded at increasing liquid recycling velocities and gas EBRTs in the absorption column. The increase in liquid recycling velocity, which entailed an increase in the wastewater loading rate in order to maintain anoxic conditions in the FBR, resulted in a slight deterioration in the removal efficiencies of organic carbon and in the denitrification of $N_2O$. The increase in the HRT in the FBR enhanced the removal performance of $N_2O$ and TOC. In our particular study, the $N_2O$ abatement performance was mainly limited by the low denitrification activity in the FBR and the $N_2O$ carrying capacity of the recycling liquid, which itself was restricted by the low aqueous $N_2O$ solubility. Innovative design and operational strategies are therefore needed to overcome the gas-liquid $N_2O$ mass transfer limitations identified in order to develop more cost efficient technologies for the abatement of $N_2O$.

## Acknowledgment

This research was supported by the Spanish Ministry of Economy and Competitiveness (CTQ2012-34949 and Red NOVEDAR CTQ2014-51693-REDC projects) and the

European Union through the Erasmus Mundus Program BABEL and FEDER Funding Program.

## References

[1] R.P.-M. Edenhofer O., Y. Sokona, S. Kadner, J. C. Minx, S. Brunner, S. Agrawala, G. Baiocchi, I. A. Bashmakov,, J.B. G. Blanco, T. Bruckner, M. Bustamante, L. Clarke, M. Conte Grand, F. Creutzig, X. Cruz-Núñez, S. Dhakal, N. K., P.E. Dubash, E. Farahani, M. Fischedick, M. Fleurbaey, R. Gerlagh, L. Gómez-Echeverri, S. Gupta, J. Harnisch, K., F.J. Jiang, S. Kartha, S. Klasen, C. Kolstad, V. Krey, H. Kunreuther, O. Lucon, O. Masera, Y. Mulugetta, R. B. Norgaard, A., N.H.R. Patt, K. Riahi, J. Roy, A. Sagar, R. Schaeffer, S. Schlömer, K. C. Seto, K. Seyboth, R. Sims, P. Smith, E. Somanathan,, C.v.S. R. Stavins, T. Sterner, T. Sugiyama, S. Suh, D. Ürge-Vorsatz, K. Urama, A. Venables, D. G. Victor, E., D.Z. Weber, J. Zou, and T. Zwickel, Technical Summary. In: Climate Change 2014: Mitigation of Climate Change, in: O. Edenhofer, R. Pichs-Madruga, Y. Sokona, E. Farahani, S. Kadner, K. Seyboth, A. Adler, I. Baum, S. Brunner, P. Eickemeier,, J.S. B. Kriemann, S. Schlömer, C. von Stechow, T. Zwickel and J.C. Minx (Eds.), Intergovernmental Panel on Climate Change, Cambridge, United Kingdom and New York, 2014. http://www.ipcc.ch/pdf/assessment-report/ar5/wg3/ipcc_wg3_ar5_technical-summary.pdf

[2] A.R. Ravishankara, J.S. Daniel, R.W. Portmann, Nitrous oxide ($N_2O$): the dominant ozone-depleting substance emitted in the 21st century, Science 326 (2009) 123-125. DOI 10.1126/science.1176985.

[3] European Environment Agency (EEA), Annual European Union greenhouse gas inventory 1990–2012 and inventory report 2014, European Environment Agency, Luxembourg, 2014. DOI 10.2800/18304

[4] P. Wunderlin, J. Mohn, A. Joss, L. Emmenegger, H. Siegrist, Mechanisms of $N_2O$ production in biological wastewater treatment under nitrifying and denitrifying conditions, Water Res. 46 (2012) 1027-1037. DOI 10.1016/j.watres.2011.11.080.

[5] M. Garzon-Zuñiga, P. Lessard, G. Aubry, G. Buelna, Nitrogen elimination mechanisms in an organic media aerated biofilter treating pig manure, Environ. Technol. 26 (2005) 361-371. DOI 10.1080/09593332608618552.

[6] R.W. Melse, J. Mosquera, Nitrous oxide ($N_2O$) emissions from biotrickling filters used for ammonia removal at livestock facilities, Water Sci. Technol. (2014) 994-1003. DOI 10.2166/wst.2013.826.

[7] M.J. Kampschreur, W.R. van der Star, H.A. Wielders, J.W. Mulder, M.S. Jetten, M.C. van Loosdrecht, Dynamics of nitric oxide and nitrous oxide emission during full-scale reject water treatment, Water Res. 42 (2008) 812-826. DOI 10.1016/j.watres.2007.08.022.

[8] K.E. Mampaey, U.G. van Dongen, M.C. van Loosdrecht, E.I. Volcke, Novel method for online monitoring of dissolved $N_2O$ concentrations through a gas stripping device, Environ. Technol. 36 (2015) 1680-1690. DOI 10.1080/09593330.2015.1005029.

[9] European Environment Agency (EEA), Trends and projections in Europe 2014: Tracking progress towards Europe's climate and energy targets for 2020, Luxembourg, 2014. DOI 10.2800/2286.

[10] K. Skalska, J.S. Miller, S. Ledakowicz, Trends in $NO_x$ abatement: a review, Sci. Total Environ. 408 (2010) 3976-3989. DOI 10.1016/j.scitotenv.2010.06.001.

[11] J.M. Estrada, N.J. Kraakman, R. Muñoz, R. Lebrero, A comparative analysis of odour treatment technologies in wastewater treatment plants, Environ. Sci. Technol. 45 (2011) 1100-1106. DOI 10.1021/es103478j.

[12] R. Jiang, S. Huang, A.T. Chow, J. Yang, Nitric oxide removal from flue gas with a biotrickling filter using *Pseudomonas putida*, J. Hazard. Mater. 164 (2009) 432-441. DOI 10.1016/j.jhazmat.2008.08.058.

[13] H. Niu, D.Y.C. Leung, C. Wong, T. Zhang, M. Chan, F.C.C. Leung, Nitric oxide removal by wastewater bacteria in a biotrickling filter, J. Environ. Sci. 26 (2014) 555-565. DOI 10.1016/s1001-0742(13)60456-8.

[14] O.D. Frutos, I.A. Arvelo, R. Perez, G. Quijano, R. Muñoz, Continuous nitrous oxide abatement in a novel denitrifying off-gas bioscrubber, Appl. Microbol. Biotechnol. 99 (2015) 3695-3706. DOI 10.1007/s00253-014-6329-8.

[15] J.C. López, G. Quijano, R. Pérez, R. Muñoz, Assessing the influence of $CH_4$ concentration during culture enrichment on the biodegradation kinetics and population structure, J. Environ. Man. 146 (2014) 116-123. DOI 10.1016/j.jenvman.2014.06.026.

[16] APHA, Standard Methods for the Examination of Water and Wastewater, twenty first ed., American Public Health Association, American Water Works Association, Water Environment Federation, 2005.

[17] R. Lebrero, E. Rodriguez, P.A. Garcia-Encina, R. Muñoz, A comparative assessment of biofiltration and activated sludge diffusion for odour abatement, J. Hazard. Mater. 190 (2011) 622-630. DOI 10.1016/j.jhazmat.2011.03.090.

[18] B.G. Hane, K. Jager, H.G. Drexler, The Pearson product-moment correlation coefficient is better suited for identification of DNA fingerprint profiles than band matching algorithms, Electrophoresis 14 (1993) 967-972. DOI 10.1002/elps.11501401154.

[19] Q. Wang, G.M. Garrity, J.M. Tiedje, J.R. Cole, Naive Bayesian classifier for rapid assignment of rRNA sequences into the new bacterial taxonomy, Appl. Environ. Microbiol. 73 (2007) 5261-5267. DOI 10.1128/aem.00062-07.

[20] S. McGinnis, T.L. Madden, BLAST: at the core of a powerful and diverse set of sequence analysis tools, Nucleic Acids Res. 32 (2004) W20-25. DOI 10.1093/nar/gkh435.

[21] S. Kim, M.A. Deshusses, Determination of mass transfer coefficients for packing materials used in biofilters and biotrickling filters for air pollution control. 1. Experimental results, Chem. Eng. Sci. 63 (2008) 841-855. DOI 10.1016/j.ces.2007.10.011.

[22] J.A. Farrar, W.G. Zumft, A.J. Thomson, $Cu_A$ and $Cu_Z$ are variants of the electron transfer center in nitrous oxide reductase, Proc Natl Acad Sci USA 95 (1998) 9891-9896.

[23] X. Zhu, Y. Chen, H. Chen, X. Li, Y. Peng, S. Wang, Minimizing nitrous oxide in biological nutrient removal from municipal wastewater by controlling copper ion concentrations, Appl. Microbiol. Biotechnol. 97 (2013) 1325-1334. DOI 10.1007/s00253-012-3988-1.

[24] R. Sander, Compilation of Henry's law constants (version 4.0) for water as solvent, Atmos. Chem. Phys. 15 (2015) 4399-4981. DOI 10.5194/acp-15-4399-2015.

[25] European Union, Urban Waste Water Treatment Directive, 91/271/EEC, 1991. http://ec.europa.eu/environment/water/water-urbanwaste/index_en.html

[26] Metcalf, I. Eddy, G. Tchobanoglous, F. Burton, H.D. Stensel, Wastewater Engineering: Treatment and Reuse, McGraw-Hill Education 2002.

[27] N. Akdeniz, K.A. Janni, I.A. Salnikov, Biofilter performance of pine nuggets and lava rock as media, Bioresour. Technol. 102 (2011) 4974-4980. DOI 10.1016/j.biortech.2011.01.058.

[28] M.C. Hood, S.B. Shah, P. Kolar, L.F. Stikeleather, Design and operation of a biofilter for treatment of swine house pit ventilation exhaust, Master Thesis, North Carolina State University, USA. (2011). http://www.lib.ncsu.edu/resolver/1840.16/7039

[29] G. MacDonald, Biogeography: Introduction to Space, Time, and Life, John Wiley and Sons 2003.

[30] J.E. Kostka, S.J. Green, L. Rishishwar, O. Prakash, L.S. Katz, L. Mariño-Ramírez, I.K. Jordan, C. Munk, N. Ivanova, N. Mikhailova, D.B. Watson, S.D. Brown, A.V. Palumbo, S.C. Brooks, Genome sequences for six *Rhodanobacter* strains, isolated from soils and the terrestrial subsurface, with variable denitrification capabilities, J. Bacteriol. 194 (2012) 4461-4462. DOI 10.1128/jb.00871-12.

[31] A. Oren, The Family *Xanthobacteraceae*, in: E. Rosenberg, E. DeLong, S. Lory, E. Stackebrandt, F. Thompson (Eds.) The Prokaryotes, Springer Berlin Heidelberg 2014, pp. 709-726.

[32] M.W. van Passel, R. Kant, A. Palva, S. Lucas, A. Copeland, A. Lapidus, T. Glavina del Rio, E. Dalin, H. Tice, D. Bruce, L. Goodwin, S. Pitluck, K.W. Davenport,

D. Sims, T.S. Brettin, J.C. Detter, S. Han, F.W. Larimer, M.L. Land, L. Hauser, N. Kyrpides, G. Ovchinnikova, P.P. Richardson, W.M. de Vos, H. Smidt, E.G. Zoetendal, Genome sequence of *Victivallis vadensis* ATCC BAA-548, an anaerobic bacterium from the phylum *Lentisphaerae*, isolated from the human gastrointestinal tract, J. Bacteriol. 193 (2011) 2373-2374. DOI 10.1128/jb.00271-11.

[33] M.N.I. Abou Seada, J.C.G. Ottow, Effect of increasing oxygen concentration on total denitrification and nitrous oxide release from soil by different bacteria, Biol. Fert. Soils. 1 (1985) 31-38. DOI 10.1007/BF00710968.

[34] F. Morgan-Sagastume, J.L. Nielsen, P.H. Nielsen, Substrate-dependent denitrification of abundant probe-defined denitrifying bacteria in activated sludge, FEMS Microbiol. Ecol. 66 (2008) 447-461. DOI 10.1111/j.1574-6941.2008.00571.x.

Figure

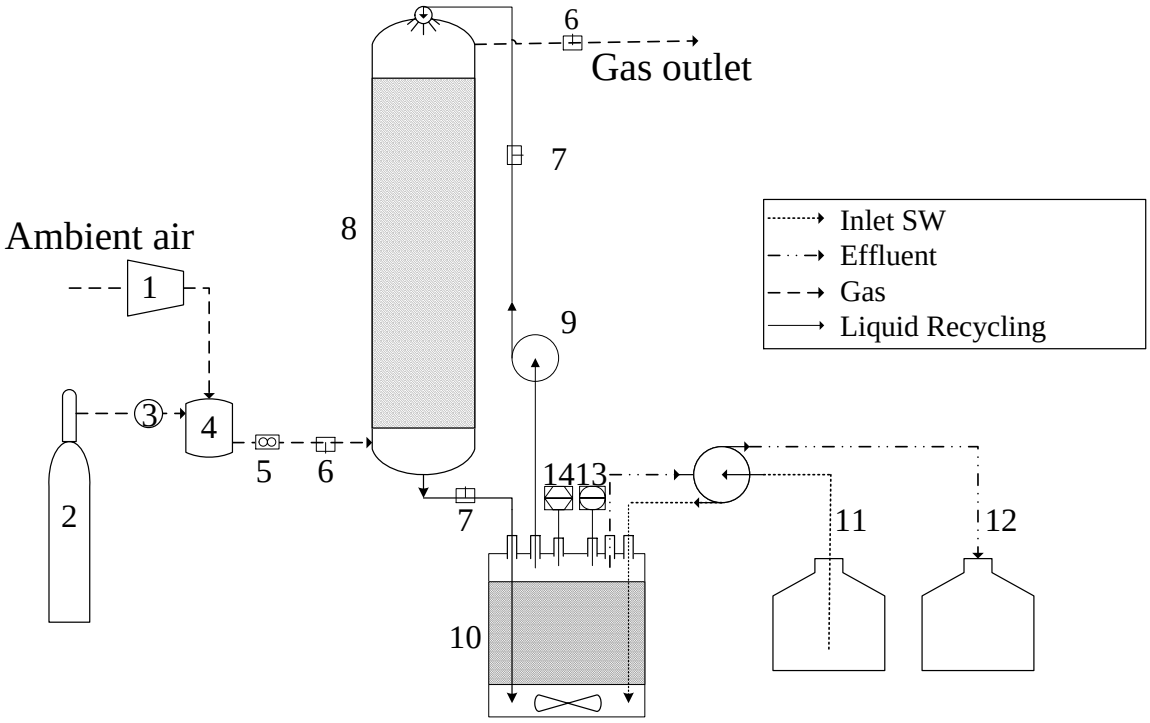


**Fig. 1.** Schematic of the bioscrubber set-up. 1) Air compressor 2) $N_2O$ reservoir 3) Mass flow controller 4) Mixing chamber 5) Gas flowmeter 6) Gas sampling port 7) Liquid sampling port 8) Absorption packed bed column 9) Liquid recycling pump 10) Denitrifying fixed bed reactor 11) Synthetic wastewater reservoir 12) Effluent storage tank 13) DO electrode 14) pH electrode.

Figure

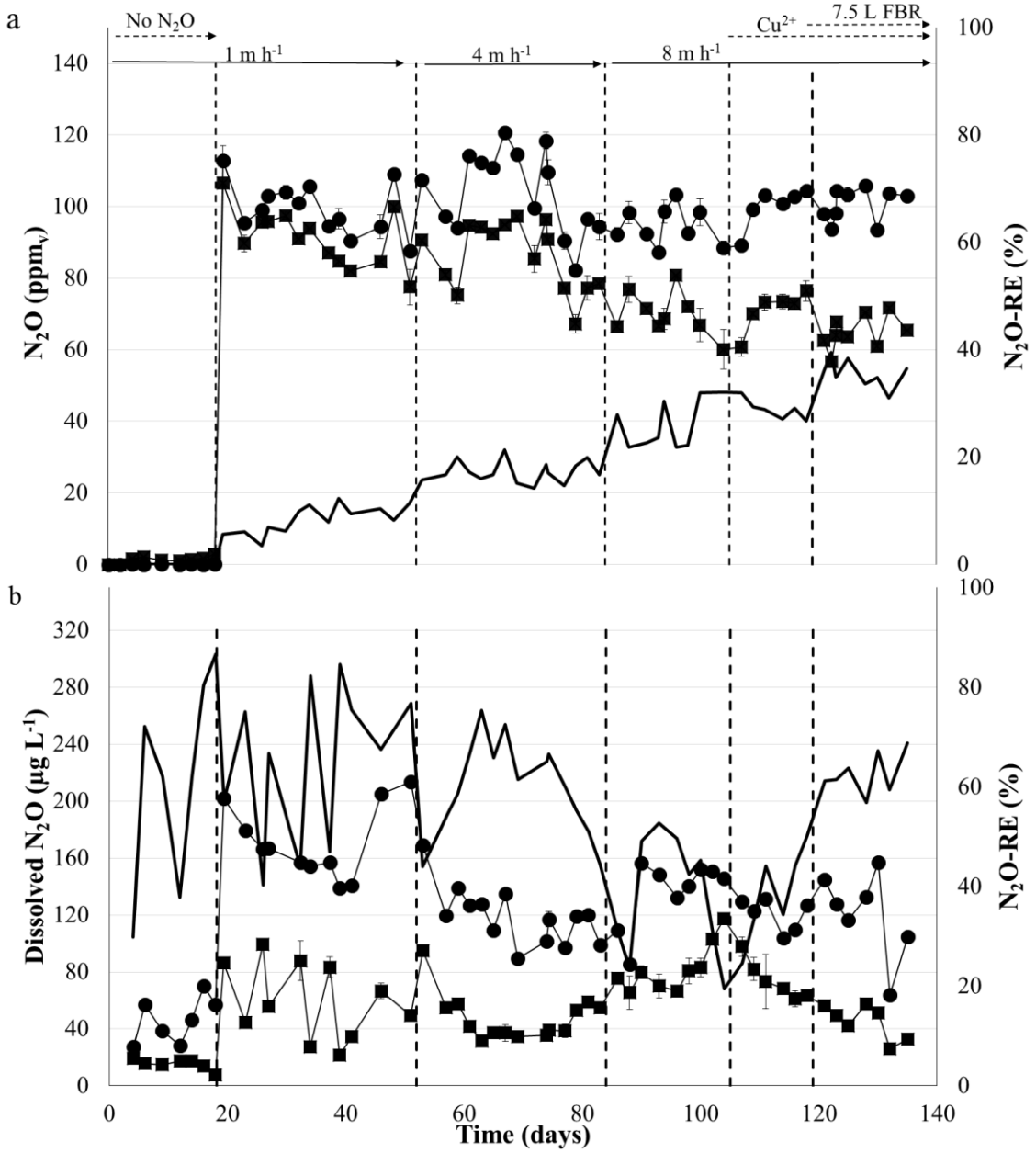


**Fig. 2.** Time course of the (a) inlet (●) and outlet (■) $N_2O$ gas concentrations and $N_2O$ removal efficiency (solid line) in the bioscrubber, and (b) inlet (●) and outlet (■) aqueous $N_2O$ concentrations and $N_2O$ removal efficiency (solid line) in the FBR. Vertical bars represent the standard deviation from duplicate measurements.

**Figure**

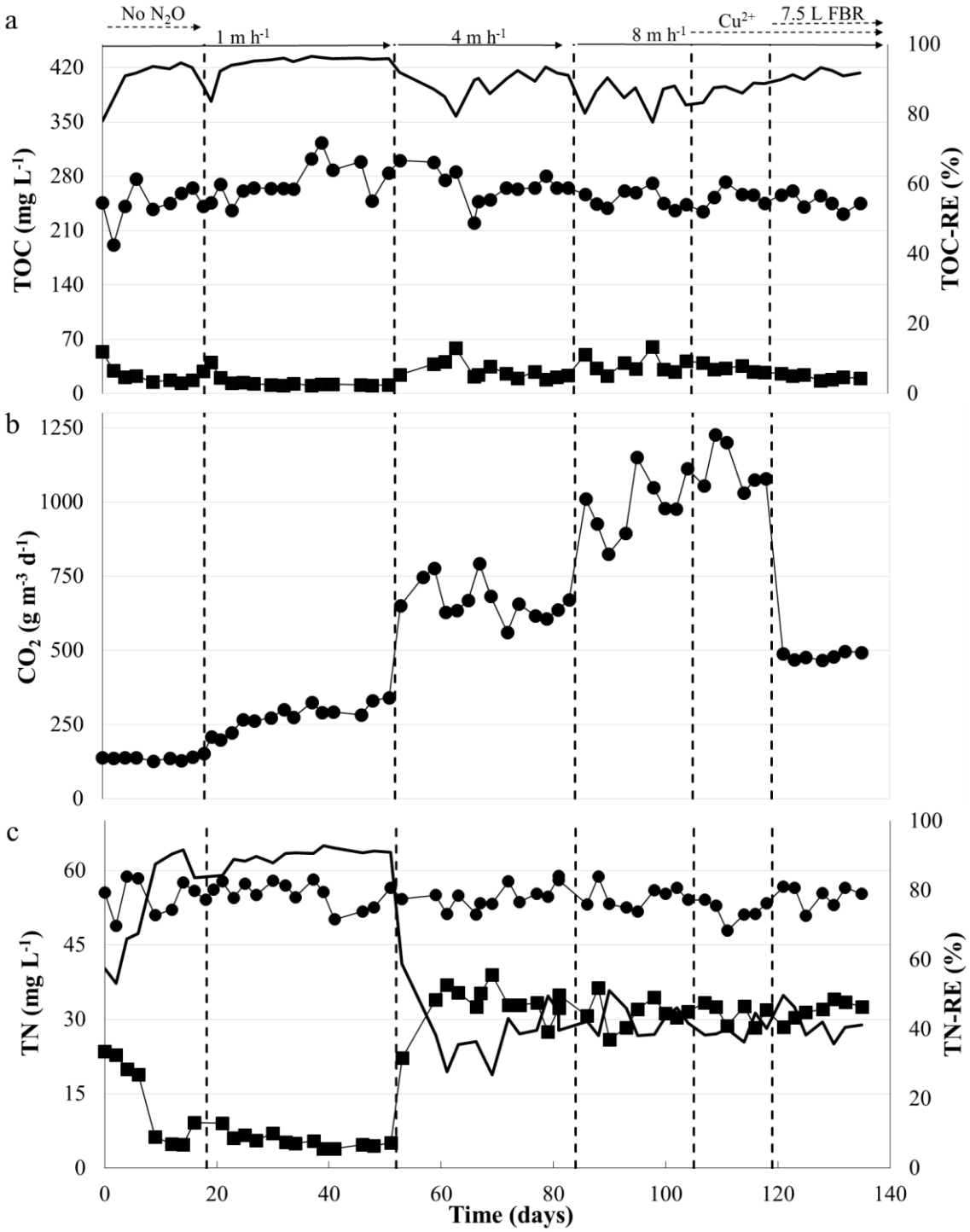


**Fig. 3.** Time course of the (a) inlet (●) and outlet (■) TOC concentrations and TOC removal efficiency (solid line) in the FBR; (b) $CO_2$ production rate (■); and (c) inlet (●) and outlet (■) TN concentrations and TN removal efficiency (solid line) in the FBR.

**Figure**

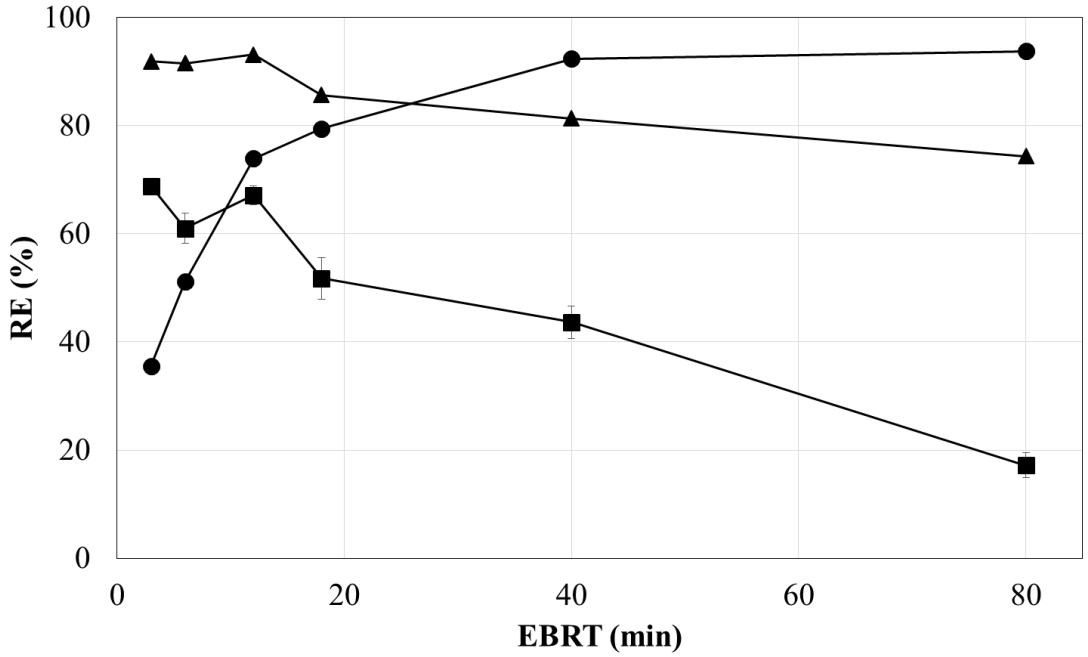


**Fig. 4.** Influence of the EBRT on the removal efficiencies of gas $N_2O$ (●), aqueous $N_2O$ (■) and total organic carbon (▲). Vertical bars represent the standard deviation from duplicate measurements.

Figure

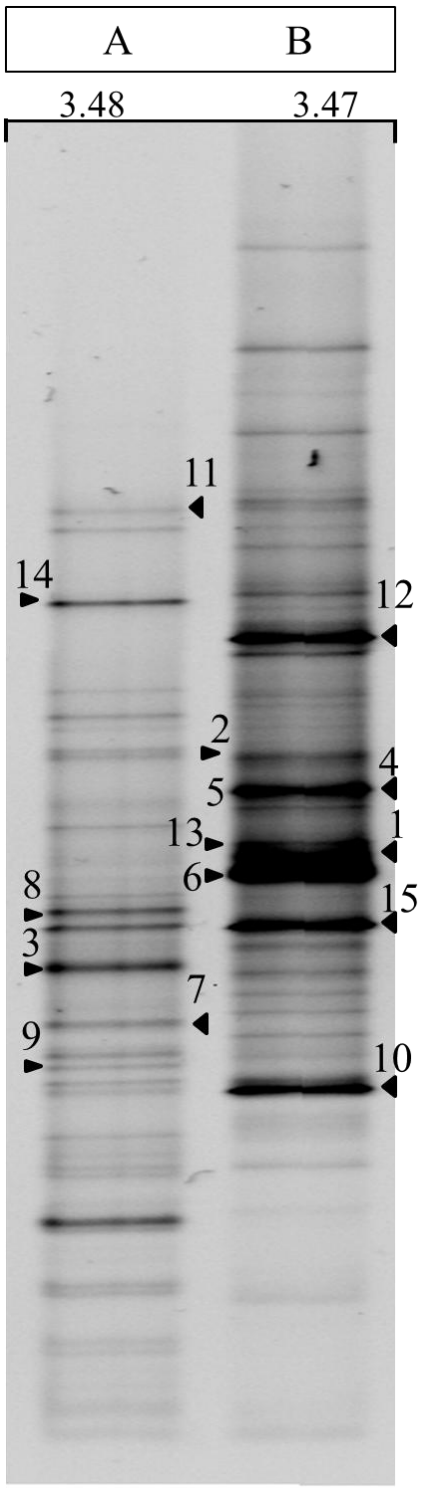


**Fig. 5.** Bacterial DGGE profiles. Sample names and Shannon diversity indices are indicated in the upper part of the gel: (A) inoculum sample, (B) FBR end operation sample. The

sequenced DGGE bands are indicated with an arrow (►) and the corresponding number of each band.

**Supplementary Material**

**Click here to download Supplementary Material: Supplementary_Material_OFrutos.docx**